Theor Chem Acc (2005) 113: 225–232
DOI 10.1007/s00214-004-0626-8

REGULAR ARTICLE

Gloria E. Moyano · Michael A. Collins

Interpolated potential energy surface for abstraction and exchange reactions of NH_3 + H and deuterated analogues

Received: 2 November 2004 / Accepted: 8 December 2004 / Published online: 5 March 2005

Abstract An ab initio interpolated potential energy surface for the hydrogen abstraction and exchange reactions between ammonia and a hydrogen atom is reported. The interpolation is constructed over a set of data points calculated at the unrestricted coupled cluster approximation, using single and double excitations, and including the triple excitations non-iteratively. New data point selection methods were used to improve the convergence and accuracy of the interpolated surface.

Keywords Potential energy surface · Reaction dynamics · Interpolation · Ammonia

1 Introduction

The hydrogen abstraction reaction

$$NH_3 + H \rightarrow NH_2 + H_2 \quad (1)$$

and its reverse,

$$NH_2 + H_2 \rightarrow NH_3 + H \quad (2)$$

have been subjects of interest in dynamics because of their role in different processes in the chemistry of ammonia, particularly in the thermal decomposition [1–10]. The investigation of these reactions has also been pursued to establish relationships with analogous hydrogen abstraction systems, some involving molecules isoelectronic with NH_3 like CH_4, H_2O and HF [7,8,11–14], or isotopic variants [7,8,11] such as

$$ND_3 + D \rightarrow ND_2 + D_2, \quad (3)$$

and the exchange reaction:

$$NH_3 + D \rightarrow NH_2D + H. \quad (4)$$

G.E. Moyano · M.A. Collins (✉)
Research School of Chemistry,
Australian National University,
Canberra ACT 0200,
Australia
E-mail: collins@rsc.anu.edu.au

This system is also of particular theoretical interest because it includes the formation of a "Rydberg" radical,

$$NH_3 + H \rightarrow NH_4, \quad (5)$$

which takes place over a barrier (see e.g. Refs. [15–19], and references cited therein). The presence of a deep minimum in the potential energy surface (PES) for NH_4 is an unusual feature in comparison with the isoelectronic CH_5 and OH_3 systems. This species is an intermediate in the exchange reaction

$$NH_3 + H' \rightarrow NH_4 \rightarrow NH_2H' + H \quad (6)$$

that can compete with reaction (1). Exchange reactions via deep intermediate wells have been predicted for ion-molecule collisions [20], but such reactions might not involve a barrier. Hence, from a theoretical viewpoint, the collision between H and NH_3 is unusual in that an abstraction reaction competes with an exchange reaction, which has a low barrier and a deep intermediate.

This paper reports a global high-level ab initio PES for the dynamical study of these competing reactions. Previously, the PES for this system has only been characterized in the vicinity of the reaction path for reactions (1) and (2). The main focus of both theoretical and experimental research on this system has been to determine the reaction rates of (1) and (2) over increasingly wider temperature ranges and to analyze the observed non-Arrhenius behavior [1–14, 21–28]. The available theoretical rate coefficients for these reactions in the ground electronic state have been determined within the framework of transition state theory (TST), variational transition state theory, and related models. The information about the PES required to apply those models has been obtained through a range of semiempirical and ab initio methods comprising the unrestricted Hartree Fock (UHF) method in the papers by Cardy et al. [22] and Leroy et al. [12]; Möller–Plesset perturbational methods, MP2, and MP4 (as reported by Barreto et al. [21]), and the spin projected variants, PMP. The perturbational methods were used along with empirical corrections such as the bond additivity correction (BAC) by Garret et al. [11]; or the scaling of all the correlation

energy (SAC4/A1) applied by Corchado and Espinosa-Garcia [24–26]. Other potential energy surface calculations for TST based rates have been performed by Mebel et al. [28] using the G2M method, and by Henon and Bohr [27] using the CASPT2 and MRSDCI approximations. An analytical form of the PES, designed to describe reactions (1) and (2) only, has been reported by Corchado and Espinosa-Garcia [23]. This surface was fitted to a combination of experimental reaction energies, enthalpies and vibrational frequencies with theoretical vibrational frequencies and energy for the transition state for reactions (1) and (2) only.

In this paper, we report two accurate PES for the dynamics of processes (1) to (6), constructed by interpolation of ab initio ground state energies, energy gradients and Hessians. The molecular configurations which form the interpolation data set for the PES are scattered over the energetically accessible regions, including the minimum energy paths (MEP) for these reactions and the NH_4 minimum. Reaction cross sections have been calculated for the classical dynamics of the reactions above. However, the classical simulations mostly serve to emphasize the need for accurate quantum dynamics. The provision of an accurate global PES for this system may facilitate such calculations.

Section 2 of this paper presents the methodology and computational details. Section 3 examines the convergence and some characteristics of the PES, and Sect. 4 reports the classical dynamics results. Finally, a discussion and a summary of this work are presented in Sect. 5.

2 Methods and computational details

2.1 Form of the PES

The PES is calculated by an iterative interpolation method whose details have been presented elsewhere [29–32]. The general form of the PES is

$$E(\mathbf{Z}) = \sum_{g\in G}\sum_{i=1}^{N_{\text{data}}} w_{goi}(\mathbf{Z})T_{goi}(\mathbf{Z}), \tag{7}$$

where a number N_{data} of local Taylor expansions T_i of the energy, around certain molecular configurations, $\mathbf{Z}(i)$, are combined as a weighted average. The N_{data} molecular configurations associated with the Taylor expansions are known as the "data set". The expansions are evaluated from ab initio calculation of the energies and up to energy second derivatives at each of the data set configurations. Each expansion is expressed in terms of a geometry-specific set of $3N$-6 independent coordinates which are linear combinations of the inverse interatomic distances, $\mathbf{Z} = Z_1, \ldots, Z_k, \ldots, Z_{N(N-1)/2}$, where $Z_k = 1/R_k$. The sum over $g \in G$ in Eq. (7) represents a sum over the symmetry group of the molecule, the complete nuclear permutation (CNP) group: if $\mathbf{Z}(i)$ is a data point, then a permuted configuration, $g \circ \mathbf{Z}(i)$ (abbreviated to $g \circ i$) is also a data point. No additional ab initio calculations are required to evaluate the Taylor series coefficients at $g \circ \mathbf{Z}(i)$, and by including all equivalent molecular configurations in Eq. (7), the PES has the correct invariance to permutation of indistinguishable nuclei $\{E(g \circ \mathbf{Z}) = E(\mathbf{Z})\}$.

The weights w_i in Eq. (7) are functions of the distance coordinates $\mathbf{Z}$ with respect to the data point configuration $\mathbf{Z}(i)$. They also depend on estimated "confidence lengths" for each data point [29, 30]. The confidence lengths for this PES were evaluated using an energy tolerance, $E_{\text{tol}} = 0.53$ kJ/mol, and energy gradients at $M = 100$ data points (see Ref. [29] for definitions of E_{tol} and M).

2.2 Iterative development of the PES

The construction of the PES and the classical trajectory simulations were performed with the program suite *Grow* [30]. The initial set of molecular configurations for the PES contained the stationary points associated with NH_4, $NH_3 + H$, $NH_2 + H_2$, and the transition state geometries for abstraction and exchange, represented in Fig. 1. The initial set also included 12 intermediate geometries along the MEP for reaction (1), and 11 points along a dissociation path for NH_4 into the fragments $NH_3 + H$. From this initial data, points are added one by one to the data set following an iterative procedure. At periodic intervals in this iteration, large scale classical trajectory simulations are performed to estimate reaction cross sections and other observable quantities, based on the current data set. The PES is taken to be converged when the calculated cross sections do not change with an increase in the number of data points.

The selection of additional data points at each iteration proceeds as follows. Classical trajectories are run to simulate the reaction [using the PES of Eq. (7)] and new data points are taken from the regions of the configuration space covered by those trajectories, using the standard criteria known as the "variance sampling" [32], and the "h-weight sampling" [30, 31, 33]. In addition, two recently proposed sampling procedures were employed to accelerate the convergence of the interpolated PES; involving the local maximization of the variance, and direct sampling of the interpolation error at four configurations in each iteration [34]. These two new criteria for selecting data points were found to result in accelerated convergence in this system.

The interpolated PES was grown from the initial set of data points to 2000 data points. The trajectories at each iteration were initiated at the transition state geometry of abstraction for 100 iterations, otherwise, for an equal number of iterations, from $NH_2 + H_2$, and from $NH_3 + H$.

2.3 Ab initio methods

The MEP, energy minima and zero point vibrational energies (ZPVE), and the classical potential barriers for Eqs. (1) and (2) have been calculated previously by several ab initio methods. The calculations performed at CCSD(T) level by Kraka et al. [14] are among the most accurate available to date. For the ammonium radical Rydberg ground state, the

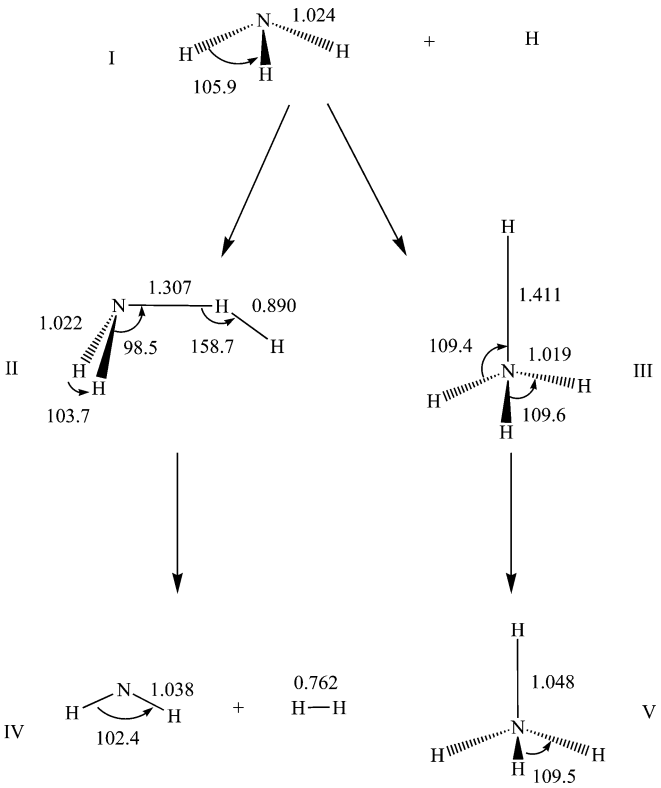

Fig. 1 The geometries of stationary configurations relevant to reactions (1)-(6) are shown. Geometries for the H_2, NH_2, NH_3, and NH_4 stable molecules resulted from UCCSD(T)/aug-cc-pVDZ geometry optimizations, while the $NH_2 \cdots H_2$ transition state was calculated at the CCSD(T)/[5s4p3d/4s3p] level by Kraka et al. [14] . The NH_4 transition state was optimized at the MP2/aug-cc-pVTZ level of theory

CCSD(T)/aug-cc-pV5Z results by Sattelmeyer et al. [35] are the highest level of optimizations reported.

In order to select the ab initio method for the interpolated PES, we computed the energy differences between all the relevant stationary geometries related to the dynamics with a range of methods and basis sets. According to the previous quantum chemistry calculations for this system, the geometries are more reproducible than the energetics for a range of ab initio methods. To compare the energetics for different basis sets and levels of theory, the molecular geometry was fixed as follows: The $NH_2 \cdots H_2$ transition state geometry is that found by Kraka et al. [14], structure II of Fig. 1; the saddle point for the exchange reaction (also the saddle point for forming NH_4) is that of structure III of Fig. 1, found by optimization at the MP2/aug-cc-pVTZ level. The remaining structures were optimized at the UCCSD(T)/aug-cc-pVDZ level. Table 1 shows the relative energies calculated here in comparison with those of other authors.

From Table 1, we see that the MP2 level of theory is inaccurate, while UQCISD is much closer to the most reliable level of theory, UCCSD(T)/aug-cc-pV5Z. The classical barrier height for reaction (1) is estimated to be about 63 kJ/mol from the UCCSD(T)/aug-cc-pV5Z calculation. The published literature values for this barrier height include an MRCI/SANO value of 66.1 kJ/mol [27], a CCSD(T)/[5s4p3d2f1g/4s3p2d1f] value of 64.4 kJ/mol [14], a HF/BAC-MP4 value of 71.5 kJ/mol [11], and a value of 65.9 kJ/mol for a minimum energy path potential constructed by Corchado and Espinosa-Garcia. Table 1 shows that the most reliable value of 63 kJ/mol is reproduced within 2 kJ/mol with the smaller aug-cc-pVDZ and aug-cc-pVTZ basis sets (62.4 and 61.4 kJ/mol, respectively).

The barrier height for the exchange reaction (6), is most reliably estimated by the UCCSD(T)/aug-cc-pV5Z value of 38.9 kJ/mol. The authors have not been able to find any estimate of this barrier height in the literature. The UCCSD(T)/aug-cc-pVDZ value overestimates the barrier height by about 3 kJ/mol, but this error is reduced to just 1.3 kJ/mol with the aug-cc-pVTZ basis set. The inclusion of diffuse basis functions is necessary to obtain reliable values for this barrier height and the energy of the nearby "Rydberg minimum". Again, Table 1 shows that the most reliable energy for the NH_4 minimum (−10.1 kJ/mol) is reproduced within 2 kJ/mol with an aug-cc-pVDZ basis, and even more accurately with the aug-cc-pVTZ basis.

Table 1 shows that the energy of the products of reaction (1) (at the equilibrium geometry) is most reliably estimated to be 23.9 kJ/mol higher than that of the reactants. The change in enthapy for this reaction, at zero Kelvin, can be estimated by adding the change in ZPVE to this value. To obtain a reliable estimate of the ZPVE of each species, we have assumed the vibrational energy levels of each mode can be approximated by

$$E(n) = \omega_e \left(n + \frac{1}{2}\right) - \omega_e x_e \left(n + \frac{1}{2}\right)^2 \tag{8}$$

The anharmonicity parameter $\omega_e x_e$ is taken to be 121 cm^{-1} for H_2, and estimated at 80 cm^{-1} for the stretching modes and zero for the bending modes. Setting the experimental vibrational frequencies [36] to $\omega_e - 2\omega_e x_e$ provides an estimate of the ZPVE for each mode. The net decrease in ZPVE for reaction (1) is thus estimated to be 13.1 kJ/mol. Using the most reliable value of 23.9 kJ/mol for ΔE_R, gives an estimated $\Delta H(0\,K)$ value of 10.8 kJ/mol. The experimental value for $\Delta H(0\,K)$, 16.2 ± 6.3 kJ/mol, has a significant uncertainty, mainly due to disagreement about the heat of formation of the NH_2 radical. Corchado and Espinosa-Garcia [23] have argued, on the basis of high level ab initio calculations, that $\Delta H(0\,K) = 8.8 \pm 3.3$ kJ/mol. Our calculations support the view that $\Delta H(0\,K)$ is near the lower limit of the experimental range. The smaller basis set calculations, UCCSD(T)/aug-cc-pVDZ and UCCSD(T)/aug-cc-pVTZ, give similar but slightly smaller values of 7.9 and 8.2 kJ/mol, respectively, in agreement with the value suggested by Corchado and Espinosa-Garcia [23].

The PES interpolation formula requires first and second derivatives of the energy, calculated here by finite differences in the energy. Since several thousand single point energies are required for the PES, we have adopted the UCCSD(T)/aug-cc-pVDZ method to calculate the surface, denoted below as PES1. However, to further improve the reliability of the surface, a second PES has been constructed wherein the

Table 1 Energy differences[a] in kJ/mol between stationary points for various ab initio methods and basis sets

	MP2[b]	UQCISD[c]	UCCSD(T)[d]	UCCSD(T)[e]	UCCSD(T)[f]	CCSD(T)[g]	CCSD[h]
ΔE_R (1)	51.3	17.0	21.0	21.3	23.9	24.6	–
ΔE_R (6)	0.8	−6.4	−8.3	−10.3	−10.1	–	−21.2
ΔE_B (1)	93.4	63.6	62.4	61.4	63.0	64.4	–
ΔE_B (5)	53.4	44.3	41.9	40.2	38.9	–	–

[a] ΔE_R denotes the energy difference between products and reactants. ΔE_B denotes the energy difference between transition state and reactants
[b,c,d] With the aug-cc-pVDZ basis set
[e] With the aug-cc-pVTZ basis set
[f] With the aug-cc-pV5Z basis set, using geometries optimized with aug-cc-VDZ for H_2, NH_2, NH_3, and NH_4
[g] Calculations by Kraka et al. [14] with basis set [5s4p3d2f1g/4s3p2d1f]
[h] Calculations by Park [18] with a triple zeta basis

energy derivatives at each data point are evaluated at the UCCSD(T)/aug-cc-pVDZ level, while the energy at each data point is calculated with a larger basis set, aug-cc-pVTZ. This surface is denoted as PES2. From the above discussion, it is clear that both PES1 and PES2 are close to the most reliable estimates of the PES at the significant stationary points on the surface. The barrier heights, in particular, are estimated with comparable or better reliability than in earlier work. No other global surfaces which describe both abstraction and exchange are available for more general comparison.

The UCCSD(T) calculations employ a Hartree–Fock (RHF) wavefunction. Convergence problems were experienced in the RHF calculation of some molecular geometries, with small to moderate differences found in the RHF energy for different initial guesses for the wavefunction. In order to overcome those problems, a routine for automatic selection of the lower energy RHF state was incorporated in the single point UCCSD(T) calculations.

The GAUSSIAN98 package [37] was used for the MP2 and the QCISD calculations, and Molpro version 2002.3 [38] for the UCCSD(T) calculations in this work. All numerical energy derivatives were evaluated with a finite difference routine implemented in *Grow*.

2.4 Classical dynamics

Interpolation data points were selected from samples of molecular configurations generated from classical trajectories. Small batches of ten trajectories were run for each iteration of the PES construction procedure to simulate collisions for either reaction (1) or (2). The trajectories were calculated with a velocity-Verlet integration algorithm, using a time step size of 1.0×10^{-17} s, starting with a fragment to fragment center of mass separation of 6.61 Å. The reactant molecules were randomly oriented and given zero rotational angular momentum. For $H + NH_3$ collisions, the relative kinetic energy was generally set at about 91.9 kJ/mol. Since this reaction has a late transition state, the reactivity of vibrationally excited molecules was explored by setting the initial vibrational energy of the NH_3 to about 144.4 kJ/mol. For the reverse reaction, the initial vibrational energy was set at 39.4 kJ/mol for H_2 and 65.6 kJ/mol for NH_2. For this reaction, the relative kinetic energy was varied from 210.0 to 262.5 kJ/mol. The initial atomic velocities and configurations for the reactants were generated using the efficient microcanonical sampling method of Schranz et al [39].

Batches of 2500 trajectories for reactions (1) and (2), were run for several sizes of the interpolation data set in order to check the convergence. For the complete PES data set, 2500 trajectories for reactions (1)–(5) were performed with vibrational energies of 89.2 kJ/mol for NH_3, 65.6 kJ/mol for ND3, 49.9 kJ/mol for NH_2, and 26.3 kJ/mol for H_2, and a range of relative kinetic energies of the fragments, in order to calculate the cross sections for these reactions. The impact parameters b for these trajectories were sampled randomly from a distribution limited by a maximum exceeding the largest value at which reaction was obtained with the given initial conditions. The distributions of b values were such that the probability of a trajectory having an impact parameter between b and $b + db$ was proportional to b.

3 Potential energy surfaces

The iterative construction process was carried out until a total of 2000 data points had been accumulated. The expectation value $\langle \mathbf{S}^2 - S_Z(S_Z + 1) \rangle$, where $\boldsymbol{S}$ and S_Z denote the total electronic spin operator for the molecule, and its component along the z axis, respectively, has an average value for the data set of 0.00305, with a standard deviation of 0.0048. This suggests that spin contamination is not a significant problem over the domain of the interpolated PES.

The convergence and accuracy of the interpolated PES1 surface was investigated as follows. The interpolation error throughout the relevant region of configuration space was examined by accumulating a sample of 3231 trajectory points from collisions between the fragments $H + NH_3$ and $NH_2 + H_2$ under the conditions used to construct the PES. The UCCSD(T)/aug-cc-pVDZ energies were evaluated for this sample and compared with the corresponding interpolated values. Figure 2 shows the evolution of the average interpolation error with the size of the data set. The decrease in the average interpolation error with data set size indicates a convergence behavior similar to that observed previously for other systems. The average interpolation error for the PES with 2000 points is below 1.70 kJ/mol, which represents about 0.75% of the energy range of configurations in the sample considered.

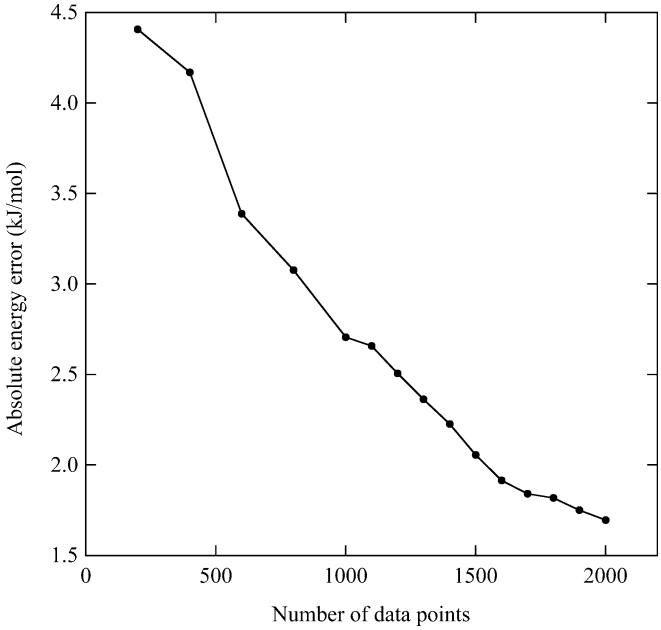

Fig. 2 The average absolute interpolation error for a random sample of 3231 trajectory configurations is shown as a function of the PES data set size

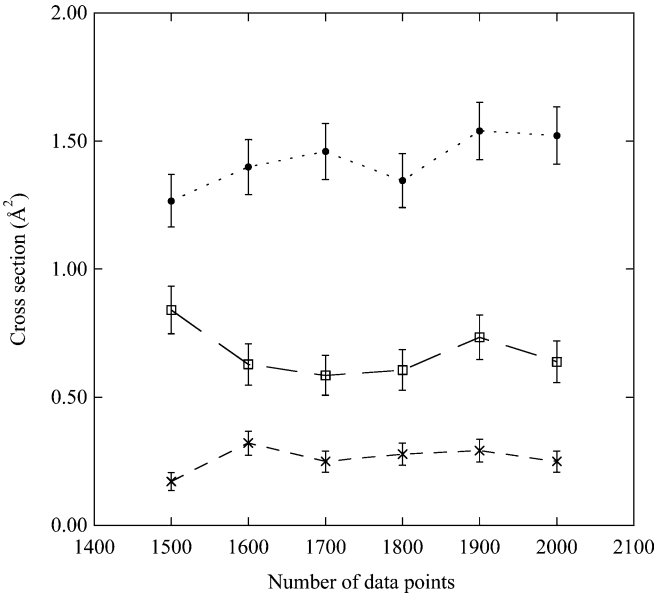

Fig. 3 Cross sections for reactions (1), •, (2), □ and (4), ×, as a function of the PES data set size. The *error bars* denote plus and minus one standard deviation expected for 2500 trajectories. The connecting lines are merely visual aids

The most relevant test of the convergence of the interpolation is the stability of observables calculated from the PES. The variation of the cross sections for reactions (1), (2) and (4) with the PES data set size is shown in Fig. 3. These cross sections were calculated from 2500 trajectories. For reaction (1), the relative kinetic energy of the fragments was 26.25 kJ/mol and the NH_3 was initially vibrationally excited to an energy of 225.75 kJ/mol. For the reverse reaction (2), the relative kinetic energy of the fragments was 131.25 kJ/mol, and the vibrational energies of NH_2 and H_2 were 136.5 and 78.75 kJ/mol, respectively. For reaction (4), the NH_3 was initially given a vibrational energy of 89.3 kJ/mol (approximately the ZPVE), and the relative translational energy was set to 131.3 kJ/mol. Clearly, the reaction cross sections are converged to within small variations for data sets approaching 2000 points.

The energy range covered by PES1 can be inferred from the energies of the data points, which are distributed as shown in the histogram in Fig. 4. The maximum in the distribution occurs at about 132.30 kJ/mol above the energy of $NH_3 + H$, and the standard deviation is 87.15 kJ/mol. There is a long tail in the distribution, extending beyond 400 kJ/mol above the $NH_3 + H$ energy.

As indicated in Sect. 2.3, a second PES was constructed by substituting the energies of each data point of the UCCSD (T)/aug-cc-pVDZ surface by the corresponding value calculated at the UCCSD(T)/aug-cc-pVTZ level. To evaluate how the basis set size affected the shape of the PES, the distribution of the differences between the UCCSD(T) energies with the aug-cc-pVTZ, and the aug-cc-pVDZ basis sets was calculated. There is an average difference of 144.93 kJ/mol between the UCCSD(T) energy values calculated with the

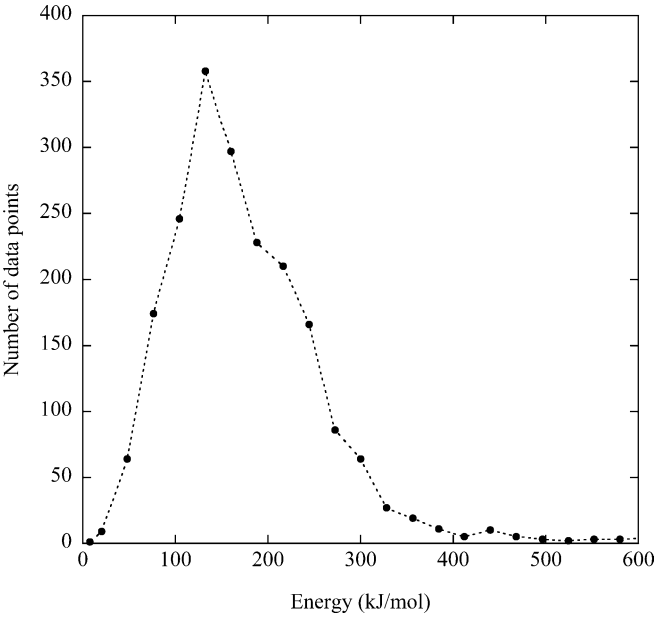

Fig. 4 This histogram depicts the distribution of the PES data point energies, relative to the energy of the separated fragments $NH_3 + H$. A bin size of 12.63 kJ/mol was used for the histogram. There is a long tail in the distribution, extending toward energies as high as 1200 kJ/mol, which has been cut for the sake of presentation

two basis sets. However, only the relative energies on each surface are relevant to the dynamics. The variation in shape of the two surfaces is indicated by the fact that the energy differences between the surfaces has a standard deviation of 6.80 kJ/mol. This should be compared with the energy range of the data (about 400 kJ/mol) as shown by Fig. 4. Table 1

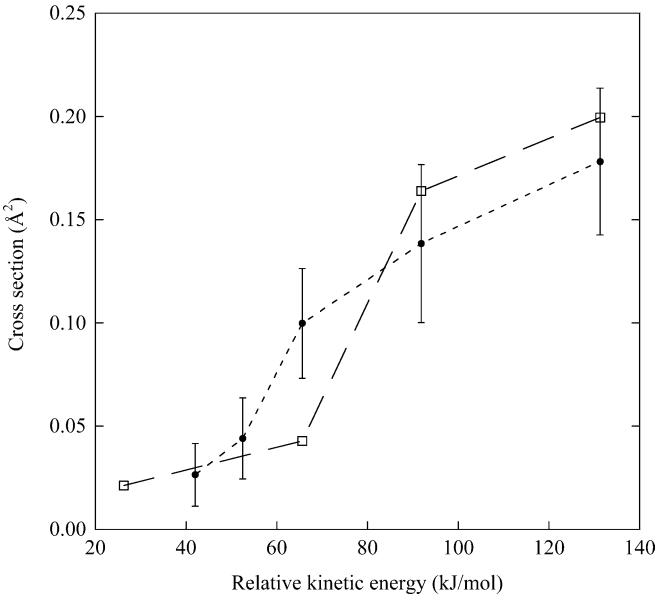

Fig. 5 The cross section for reaction (1) for PES1 (•) and PES2 (□) is shown as a function of the relative kinetic energy of the reactants. The initial vibrational energy of NH_3 was 89.3 kJ/mol. The *error bars* denote plus and minus one standard deviation expected for 2500 trajectories

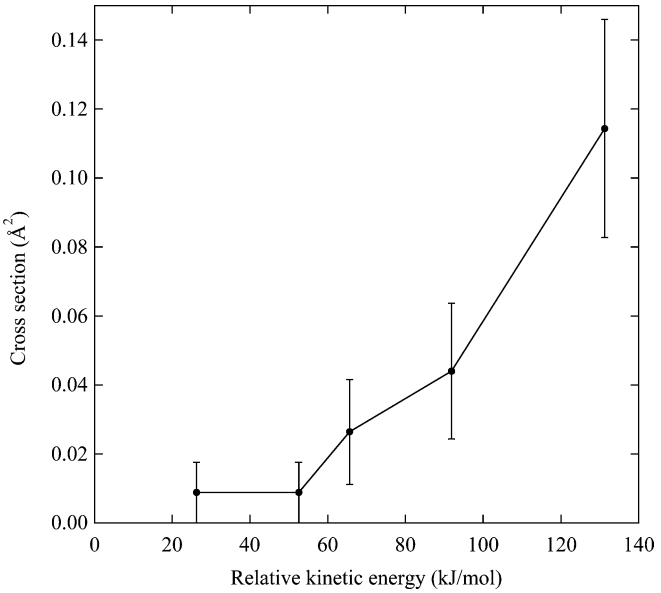

Fig. 6 The cross section for reaction (3), for PES1, is shown as a function of the relative kinetic energy of the reactants. The initial vibrational energy of ND_3 was 65.6 kJ/mol. The *error bars* denote plus and minus one standard deviation expected for 2500 trajectories

also indicates that the reaction barriers and reaction energies vary by only a few kJ/mol with this change in basis set.

4 Dynamics of exchange and abstraction reactions

To give a qualitative view of the reaction dynamics on these surfaces, classical simulations for the collisions of $NH_3 + H$, $NH_2 + H_2$, $NH_3 + D$, and $ND_3 + D$ have been performed, as described in Sect. 2.4.

4.1 Abstraction reactions (1), (2) and (3)

The total cross sections for these reactions are shown in Figs. 5–7 as functions of the relative kinetic energy of the reactants. Figure 5 presents the cross section for reaction (1) when the NH_3 reactant has near zero point vibrational energy (ZPVE≈89.3 kJ/mol). The cross sections are very small, even when the translational energy is more than 70 kJ/mol above the classical barrier height. The statistical uncertainty in these classical cross sections is therefore relatively large. In the light of this, we cannot definitively distinguish between the cross sections for PES1 and PES2. Note that the classical barrier height is about 60 kJ/mol for both PES1 and PES2. Hence, Fig. 5 indicates that the classical cross sections are above 0.02 Å^2 at energies well below the barrier height. No doubt the substantial ZVPE in NH_3 is promoting the reaction in these classical simulations.

The cross section for the deuterated analogue, reaction (3), increases with increasing relative kinetic energy in a fashion similar to that seen for reaction (1). Figure 6 presents the cross section for this reaction on PES1, where ND_3 has an initial vibrational energy of 65.6 kJ/mol, corresponding to its ZPVE. The cross section for reaction (3) is lower than that of (1) at the same relative kinetic energy.

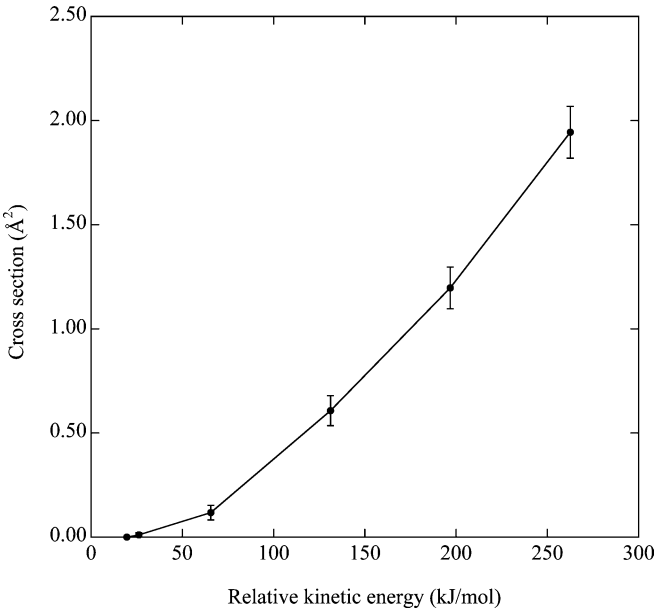

Fig. 7 The cross section for reaction (2), for PES1, is shown as a function of the relative kinetic energy of the reactants. The initial vibrational energies of NH_2 and H_2 were 49.9 and 26.3 kJ/mol, respectively. The *error bars* denote plus and minus one standard deviation expected for 2500 trajectories

Figure 7 shows the reactive cross section for collisions between NH_2 and H_2 in which the fragments have near zero point vibrational energies (49.9 kJ/mol for NH_2 and 26.3 kJ/mol for H_2). The cross section is about an order of

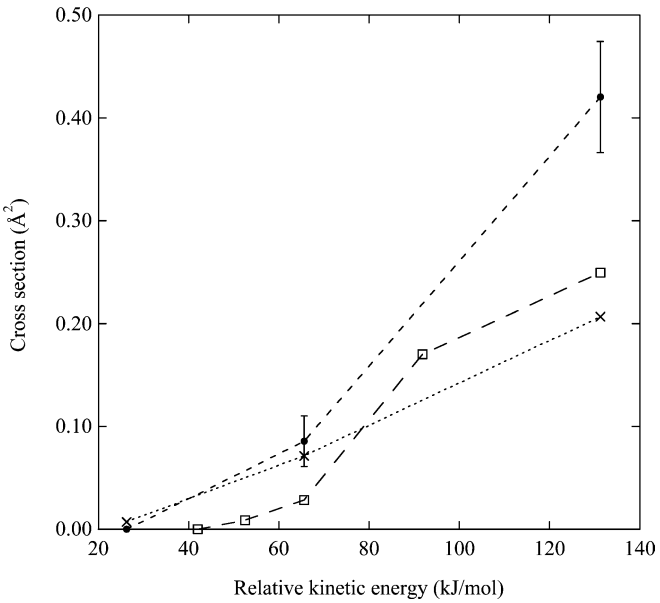

Fig. 8 The cross sections for reaction (4), (•), and (5), (□), and $NH_3 + D \rightarrow NH_2 + HD$, (×), for PES1, are shown as a function of the relative kinetic energy of the reactants. The initial vibrational energy of NH_3 was 89.3 kJ/mol. The *error bars* denote plus and minus one standard deviation expected for 2500 trajectories

magnitude larger than that for reaction (1) at the same translational energy.

4.2 Exchange reactions (4) and (5)

The cross sections for the exchange reactions in $D + NH_3$ and $H + NH_3$ on PES1 are shown in Fig. 8. The cross section for abstraction, $D + NH_3 \rightarrow DH + NH_2$, is also shown for comparison. In all reactions, the NH_3 fragment has approximately the ZVPE of 89.3 kJ/mol. No reactive trajectories for the exchange reaction were observed for a relative kinetic energy below 42 kJ/mol, which corresponds to the classical barrier. Although the reaction cross section for H/D exchange is small, it exceeds that for hydrogen abstraction by a factor near two. Although the statistical uncertainty in these small cross section is relatively large, the deuterium exchange reaction (4) appears to have a larger cross section than that for H atom exchange, (5).

5 Concluding remarks

Two interpolated energy surfaces, denoted PES1 and PES2, have been constructed for NH_4 at the UCCSD(T) level of ab initio theory. The surfaces were constructed with data point geometries accumulated from trajectories for the abstraction reaction (1), the corresponding reverse reaction (2), and the exchange reaction (5). The configuration space was explored for reactions involving highly excited reactants, and translational energies up to about 92 kJ/mol for reaction (1) and about 260 kJ/mol for reaction (2). The average interpolation error for PES1 is estimated to be about 1.7 kJ/mol over an energy range of about 226 kJ/mol. PES2 was constructed from PES1 by replacing the data point energies by values obtained with a larger basis set. Although the two surfaces are quantitatively different, the resultant classical cross sections for the abstraction reaction (1) are very similar.

The classical simulations reported here indicate that quantum dynamics would be necessary to describe the reaction cross sections near threshold. These surfaces should be suitable for quantum studies of these reactions, including the reactions of vibrationally excited species. The quantitative differences between PES1 and PES2 may be more apparent in quantum scattering at low energy where differences in the barrier heights would have a significant effect on tunneling. Given that the surfaces reported here are evaluated from first principles, with no empirical scaling, exact quantum dynamics is required to complete the comparison between theory and experiment for reaction cross sections and thermal rate coefficients. However, for translational energies well above the threshold, the classical cross sections for abstraction and exchange have been shown to be accurate in the analogous $H + H_2O$ and $H + N_2O$ systems [40,41]. Hence, the cross sections in Figs. 5–8 at high energy should be directly comparable with experimental data (when available).

In addition to the chemical significance of these reactions, this system is of particular theoretical interest because of the unusual topology of the PES. There is relatively deep well on the surface associated with a tetrahedral NH_4 structure, which results from the partial Rydberg character of the electronic ground state. In the isoelectronic OH_3 system, the same electronic effect produces only a very shallow minimum at the top of a high barrier for the exchange reaction. The "Rydberg effect" is much stronger in NH_4, producing an energy minimum (neglecting ZPVE) below the energy of the separated species, $H + NH_3$. The barrier to exchange in $H + H_2O$ is near 90 kJ/mol, and only about 40 kJ/mol for $H + NH_3$. For the competing abstraction reactions, the barriers are about 90 kJ/mol for $H + H_2O$ and about 60 kJ/mol for $H + NH_3$.

For $H + H_2O$, the exchange cross section is about a factor of 10–20 larger than that for abstraction at energies well above the (coincidentally) similar barriers to reaction. For $H + NH_3$, this factor is nearer two, even though the barrier to exchange is about 20 kJ/mol lower than that for abstraction. However, it is important to note that these observations, for $H + NH_3$, are based only on classical dynamics. The quantum effect of the deep "Rydberg" well on the cross section for exchange in $H + NH_3$ is yet to be discovered.

The software and data for PES1 and PES2 are available as EMS documents. The *Grow* software can be provided by the authors on request.

Acknowledgements The authors wish to thank the Australian Partnership for Advanced Computing National Facility for an allocation of computer time, and Prof. H.-J. Werner for helpful suggestions with regard to the RHF calculations.

References

1. Friedrichs G, Wagner HG (2000) Zeit fur Physikalische Chemie 214:1151
2. Willis C, Boyd AW, Miller OA (1969) Can J Chem 47:3007
3. Dove JE, Nip WS (1974) Can J Chem 52:1171
4. Demissy M, Lesclaux R (1980) J Am Chem Soc 102:2897
5. Michael JV, Sutherland JW, Klemm RB (1986) J Phys Chem 90:497
6. Hack W, Rouveirolles P, Wagner HG (1986) J Phys Chem 90:2505
7. Marshall P, Fontijn A (1986) J Chem Phys 85:2637
8. Marshall P, Fontijn A (1987) J Phys Chem 91:6297
9. Sutherland JW, Michael JV (1988) J Chem Phys 88:830
10. Ko T, Marshall P, Fontijn A (1990) J Phys Chem 94:1401
11. Garrett B, Koszykowski M, Melius C, Page M (1990) J Phys Chem 94:7096
12. Leroy G, Sana M, Tinant A (1984) Can J Chem 63:1447
13. Gordon MS, Gano DR, Boatz JA (1983) J Am Chem Soc 105:5771
14. Kraka E, Gauss J, Cremer D (1993) J Chem Phys 99:5306
15. Cardy H, Liotard D, Dargelos A (1983) Chem Phys 77:287
16. Chen FW, Davidson ER (2001) J Phys Chem A 105:10915
17. Kassab E, Evleth EM (1987) J Am Chem Soc 109:1653
18. Park JK (1997) J Chem Phys 107:6795
19. Park JK (1998) J Chem Phys 109:9753
20. Fuller RO, Bettens RPA, Collins MA (2001) J Chem Phys 114:10711
21. Barreto P, Alessandra FA, Gargano R (2003) J Mol Struct (Theochem) 639:167
22. Cardy H, Liotard D, Dargelos A (1980) Nouveau J de Chimie 4:751
23. Corchado JC, Espinosa-Garcia J (1997) J Chem Phys 106:4013
24. Espinosa-Garcia J, Corchado JC (1994) J Chem Phys 101:1333
25. Espinosa-Garcia J, Tolosa S, Corchado JC (1994) J Phys Chem 98:2337
26. Espinosa-Garcia J, Corchado JC (1997) J Phys Chem A 101:7336
27. Henon E, Bohr F (2000) J Mol Struct (Theochem) 531:283
28. Mebel AM, Moskaleva LV, Lin MC (1999) J Mol Struct (Theochem) 461–462:223
29. Bettens RPA, Collins MA (1999) J Chem Phys 111:816
30. Collins MA (2002) Theor Chem Acc 108:313
31. Jordan MJT, Thompson KC, Collins MA (1995) J Chem Phys 102:5647
32. Thompson KC, Collins MA (1997) J Chem Soc Faraday Trans 93:871
33. Ischtwan J, Collins MA (1994) J Chem Phys 100:8080
34. Moyano GE, Collins MA (2004) J Chem Phys 121:9769
35. Sattelmeyer KW, Schaefer III HF, Stanton JF (2001) J Chem Phys114:9863
36. NIST Chemistry WebBook (March, 2003) http://webbook.nist.gov/chemistry/
37. Frisch GW, Trucks GW, Schlegel HB, Scuseria GE, Robb MA, Cheeseman JR, Zakrzewski VG, Montgomery J, Stratmann RE, Burant JC, Dapprich S, Millam JM, Daniels AD, Kudin KN, Strain MC, Farkas O, Tomasi J, Barone V, Cossi M, Cammi R, Mennucci B, Pomelli C, Adamo C, Clifford S, Ochterski J, Petersson GA, Ayala PY, Cui Q, Morokuma K, Malick DK, Rabuck AD, Raghavachari K, Foresman JB, Cioslowski J, Ortiz JV, Stefanov BB, Liu G, Liashenko A, Piskorz P, Komaromi I, Gomperts R, Martin RL, Fox DJ, Keith T, Al-Laham MA, Peng CY, Nanayakkara A, Gonzalez C, Challacombe M, Gill PMW, Johnson B, Chen W, Wong MW, Andres JL, Gonzalez C, Head-Gordon M, Replogle ES, Pople JA (1998) GAUSSIAN 98 Revision A.6 (Gaussian Inc., Pittsburgh)
38. Amos RD, Bernhardsson A, Berning A, Celani P, Cooper DL, Deegan MJO, Dobbyn AJ, Eckert F, Hampel C, Hetzer G, Knowles PJ, Korona T, Lindh R, Lloyd AW, McNicholas SJ, Manby FR, Meyer W, Mura ME, Nicklass A, Palmieri P, Pitzer R, Rauhut G, Schütz M, Schumann U, Stoll H, Stone AJ, Tarroni R, Thorsteinsson T, Werner H-J (2002) MOLPRO version 2002.3
39. Schranz HW, Nordholm S, Nyman G (1991) J Chem Phys 94:1487
40. Brouard M, Burak I, Minayev D, O'Keeffe P, Vallance C, Aoiz FJ, Banares L, Castillo JF, Zhang DH, Collins MA (2003) J Chem Phys 118:1162
41. Castillo JF, Aoiz FJ, Banares L, Collins MA (2004) J Phys Chem A 108:6611